

Supplementary Material

On the Stability of Peptide Nucleic Acid Duplexes in the presence of Organic Co-solvents

Anjana Sen and Peter E. Nielsen*

*Department of Cellular and Molecular Medicine,
Faculty of Health Sciences, The Panum Institute,
University of Copenhagen,
Blegdamsvej 3c, 2200 Copenhagen N, Denmark
E-mail: pen@imbg.ku.dk*

List of Tables in the supplementary

Table S1: List of the PNA and DNA sequences studied.

Table S2: Thermal and thermodynamic parameters of PNA1·PNA2, PNA1·DNA2 and DNA1·DNA2 duplexes in DMF.

Table S3: Thermal and thermodynamic parameters of longer DNA duplex control DNA3·DNA4 in DMF and dioxane.

Table S4: Comparison of T_m and ΔG_{37}^0 values of PNA1·PNA2, PNA1·DNA2, PNA2·DNA1 and DNA1·DNA2 duplexes in DMF and dioxane.

Table S5: Thermal and thermodynamic parameters of PNA1·PNA2 and DNA3·DNA4 duplexes in formamide.

Table S6: Thermal and thermodynamic parameters of hairpin PNAs PNA3 and PNA4 in DMF.

Table S7: Thermal and thermodynamic parameters of hairpin PNAs PNA3 and PNA4 in dioxane.

Table S8: Thermal and thermodynamic parameters of hairpin DNA control DNA5 in DMF.

Table S9: Thermal and thermodynamic parameters of hairpin DNA control DNA5 in dioxane.

Table S10: Thermal and thermodynamic parameters of PNA duplexes PNA5·PNA6 containing tricyclic thymine (tT) and its control duplex PNA6·PNA7 in DMF.

Table S11: T_m and ΔG_{37}^0 values of single base mismatched PNA duplexes PNA1·PNA8 (T·T mismatch), PNA2·PNA9 (A·A mismatch) and PNA2·PNA10 (C·T mismatch) in DMF.

List of figures in the supplementary

Figure S1: Representative thermal melting curves of PNA and DNA duplexes in aqueous buffer.

Figure S2: Representative thermal melting curves of PNA1·PNA2 in increasing concentration of (A) DMF and (B) dioxane.

Figure S3: Representative thermal melting curves of DNA3·DNA4 in increasing concentration of (A) DMF and (B) dioxane.

Figure S4: Plots of (A) T_m and (B) ΔG_{37}^0 of PNA1·PNA2 as a function of the amount of DMF and dioxane.

Figure S5: Plots of (A) T_m and (B) ΔG_{37}^0 of PNA1·DNA2 as a function of the amount of DMF and dioxane.

Figure S6: Representative thermal melting curves of (A) PNA1·PNA2 and (B) DNA3·DNA4 in increasing concentration of formamide.

Figure S7: Plots of (A) T_m , (B) ΔG_{37}^0 , (C) ΔH^0 and (D) ΔS^0 of PNA1·PNA2 as a function of the amount of formamide.

Figure S8: Plots of (A) T_m , (B) ΔG_{37}^0 , (C) ΔH^0 and (D) ΔS^0 of DNA3·DNA4 as a function of the amount of formamide.

Figure S9: Plots of (A) ΔG_{37}^0 , (B) ΔH^0 and (C) ΔS^0 of hairpin PNAs PNA3 and PNA4 as a function of the amount of DMF and dioxane.

Figure S10: Plots of T_m values of hairpin DNA control DNA5 as a function of the amount of (A) DMF and (B) dioxane.

Figure S11: Plots of (A) T_m and (B) ΔG_{37}^0 of PNA5·PNA6 and PNA6·PNA7 as a function of the amount of DMF.

Figure S12: Plots of T_m and ΔG_{37}^0 of PNA1·PNA8 (T·T mismatch, A and B) and PNA2·PNA9 (A·A mismatch, C and D) as a function of the amount of DMF.

Figure S13: Plots of (A) T_m and (B) ΔG_{37}^0 of PNA2·PNA10 (C·T mismatch) as a function of the amount of DMF.

Table S1 PNA and DNA sequences.

Name	Sequence ^{a, b}	Base composition	ϵ_{260} ($M^{-1}cm^{-1}$)
PNA1	H-GTA GAT CAC T-Lys-NH ₂	A ₃ G ₂ T ₃ C ₂	110600
PNA2	H-AGT GAT CTA C-Lys-NH ₂	A ₃ G ₂ T ₃ C ₂	110600
PNA3	H-AGAG-(eg1) ₃ -CTCT-Lys-NH ₂	A ₂ G ₂ T ₂ C ₂	86400
PNA4	H-ACAG-(eg1) ₃ -CTGT-Lys-NH ₂	A ₂ G ₂ T ₂ C ₂	86400
PNA5	H-tT-GTA GAT CAC T-NH ₂	A ₃ G ₂ T ₃ fTC ₂	119400
PNA6	H-AGT GAT CTA C-NH ₂	A ₃ G ₂ T ₃ C ₂	110600
PNA7	H-GTA GAT CAC T-NH ₂	A ₃ G ₂ T ₃ C ₂	110600
PNA8	H-AGT GTT CTA C-Lys-NH ₂	A ₂ G ₂ T ₄ C ₂	104200
PNA9	H-GTA GAA CAC T-Lys-NH ₂	A ₄ G ₂ T ₂ C ₂	117600
PNA10	H-GTA GCT CAC T-Lys-NH ₂	A ₂ G ₂ T ₃ C ₃	102700
DNA1	5'-GTA GAT CAC T-3'	A ₃ G ₂ T ₃ C ₂	100300
DNA2	5'-AGT GAT CTA C-3'	A ₃ G ₂ T ₃ C ₂	100700
DNA3	5'-AGT GAT CTA CGG TGG ACG GTC C-3'	A ₄ G ₈ T ₃ C ₅	213700
DNA4	5'-GGA CCG TCC ACC GTA GAT CAC T-3'	A ₅ G ₅ T ₄ C ₈	208300
DNA5	5'-AGA GTT TTC TCT-3'	A ₂ G ₂ T ₆ C ₂	111700

- a. All the duplexes resulting from these sequences would be antiparallel (either N/C or N/3' or 5'/3').
- b. The N-terminal of the peptide backbone of PNA is shown by an 'H' and the amidated carboxyl terminal of the peptide backbone of PNA is shown by an 'NH₂'.

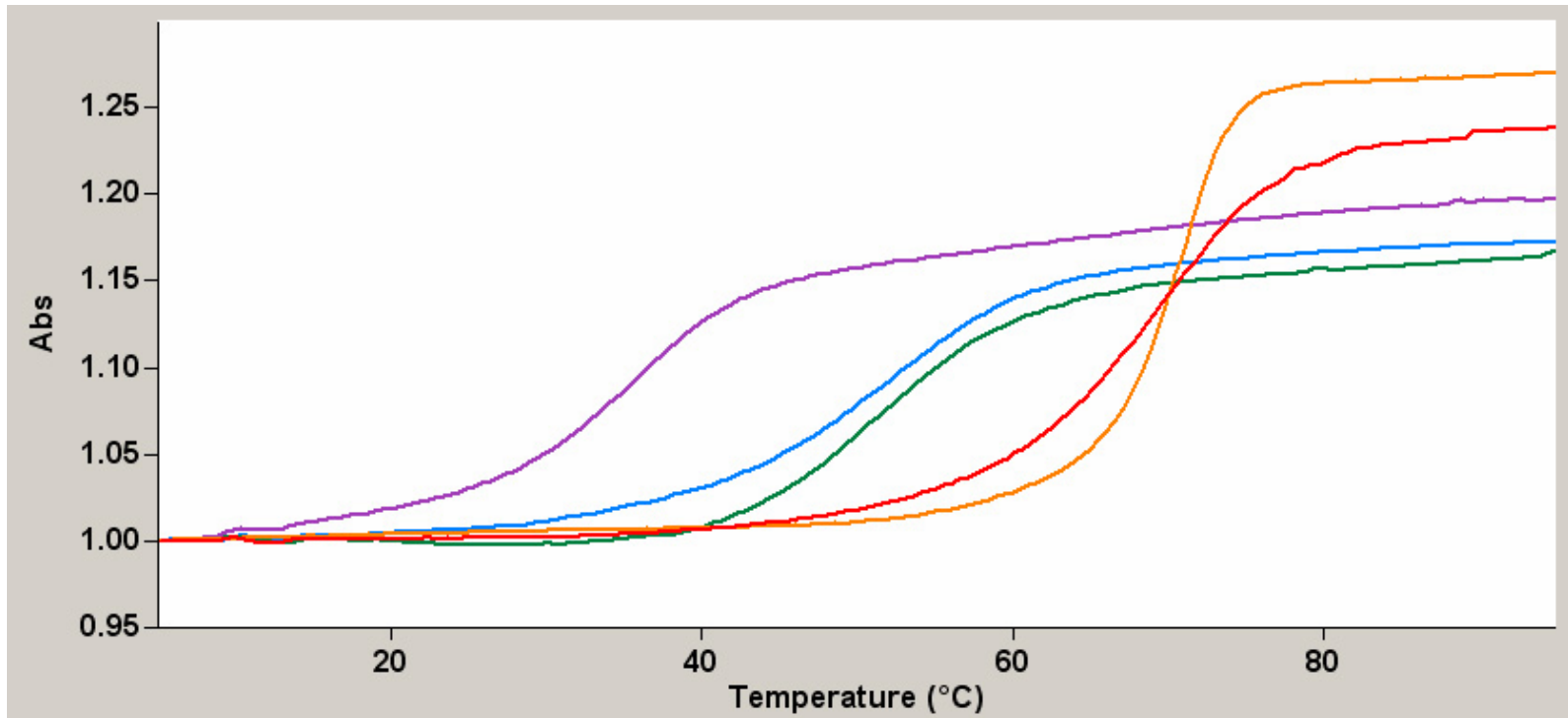


Figure S1

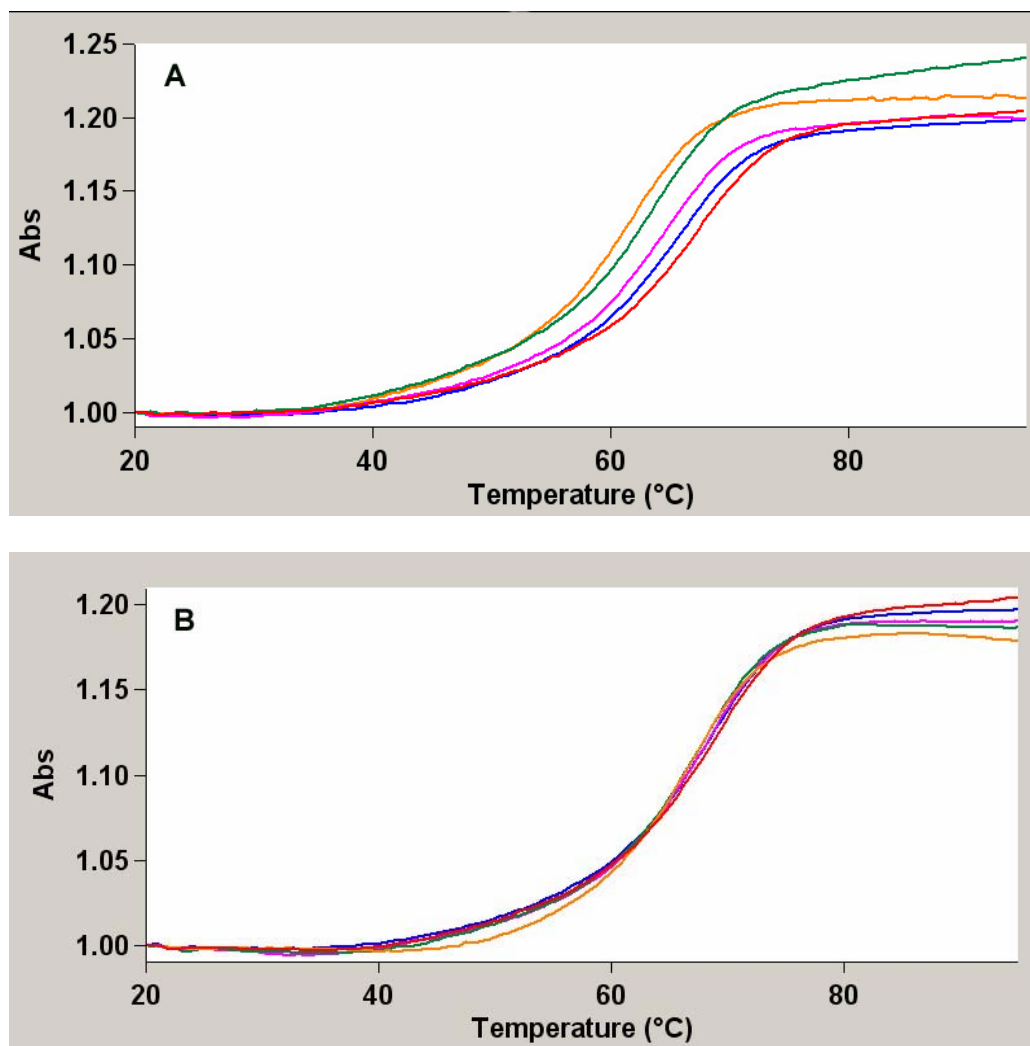


Figure S2

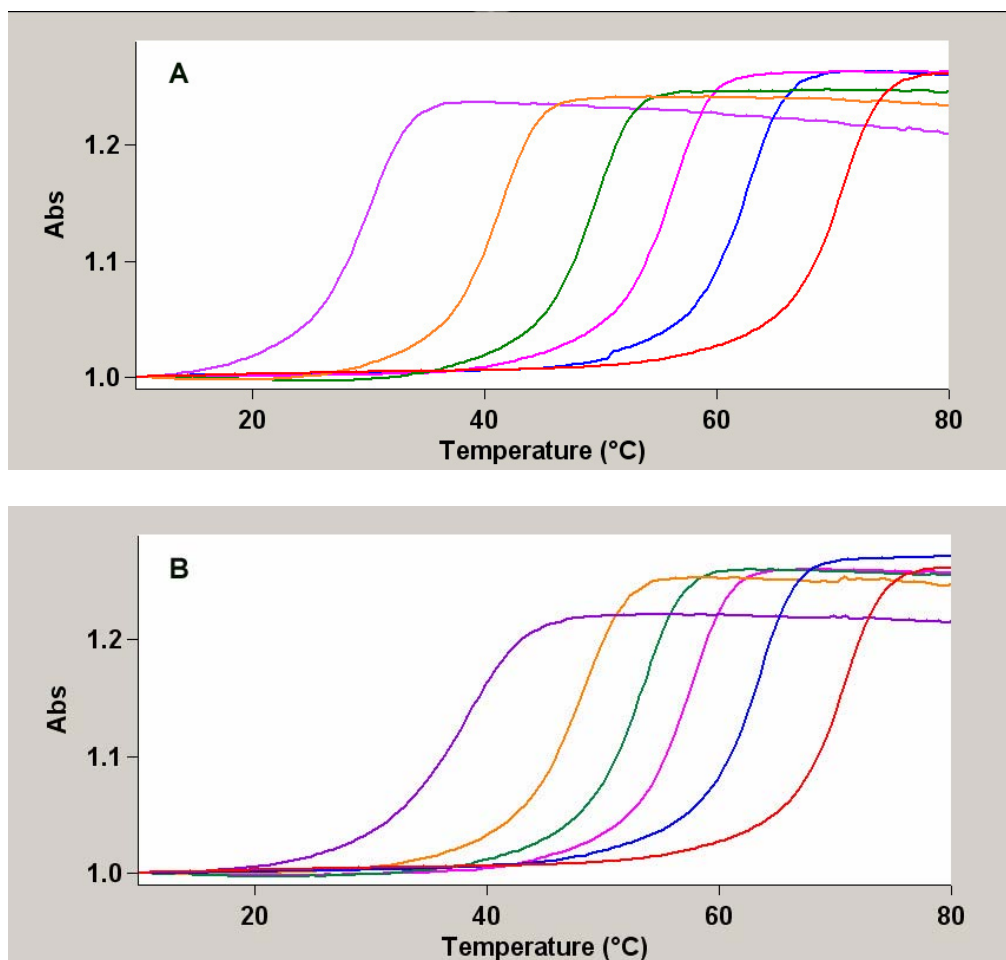


Figure S3

Table S2 Thermal and thermodynamic parameters of PNA and DNA duplexes in DMF.

Solvent effect on PNA1-PNA2							
DMF (%)	T_m (°C) ^{a, b}	Concentration method			Hyperchromicity method		
		ΔG_{37}^0 (kcal/mol)	ΔH^0 (kcal/mol)	ΔS^0 (cal/mol.K)	ΔG_{37}^0 (kcal/mol) ^b	ΔH^0 (kcal/mol) ^b	ΔS^0 (cal/mol.K) ^b
0	70.2±0.3	-17.2	-96.9	-256.9	-16.6±0.5	-93.8±4.7	-249.0±11.4
10	68.3±0.2	-16.2	-91.1	-241.3	-15.4±0.5	-81.1±3.8	-213.9±10.6
20	66.2±0.2	-15.6	-88.3	-234.2	-14.3±0.4	-80.9±5.2	-214.9±9.8
30	64.3±0.5	-15.7	-94.6	-254.3	-14.5±0.8	-84.7±3.2	-226.4±11.8
40	63.4±0.3	-15.9	-98.8	-267.2	-14.4±0.5	-89.7±4.6	-241.8±12.1
50	61.3±0.4	-15.5	-98.4	-267.5	-13.6±0.7	-82.4±5.0	-238.2±10.8
Solvent effect on DNA1-DNA2							
0	35.8±0.5	-7.9	-69.0	-197.6	-8.2±0.7	-71.0±3.5	-202.4±8.8
10	29.2±0.4	-6.1	-67.3	-196.3	-6.2±1.2	-64.0±5.0	-186.1±9.5
20	23.7±0.5	-4.9	-65.0	-194.0	-4.9±0.8	-65.6±4.7	-195.0±12.0
30 ^d	18.2±0.3	-3.9	-63.9	-193.5	-3.7±0.5	-64.2±5.0	-195.0±9.6
Solvent effect on PNA1-DNA2							
0	51.3±0.4	-11.3	-73.3	-199.9	-10.3±1.0	-70.5±3.2	-193.9±12.3
10	47.0±0.5	c	c	c	-9.5±0.7	-57.8±4.5	-155.8±10.0
20	43.1±0.3	c	c	c	-9.0±0.6	-61.7±4.4	-169.9±10.6
30	40.2±0.4	c	c	c	-8.3±0.6	-59.1±5.2	-163.8±11.8
40	36.2±0.5	c	c	c	-7.7±0.8	-59.7±3.8	-167.4±9.7
50	31.1±0.2	-6.8	-61.1	-174.7	-6.7±0.5	-56.7±4.2	-161.0±12.0

a. PNA duplex concentration was 5.0μM in strands.

b. Five independent measurements were used to calculate the standard deviation.

c. Data were not measured, as the data evaluated from the other method was sufficient to give necessary information.

d. Data at higher than 30% of DMF could not be measured because of incomplete thermal melting curves (too low melting temperature).

Table S3 Thermal and thermodynamic parameters^a of longer DNA duplex control DNA3·DNA4 in DMF and dioxane.

DMF (%)	T _m (°C) ^{b, c}	ΔG ₃₇ ⁰ (kcal/mol) ^c	ΔH ⁰ (kcal/mol) ^c	ΔS ⁰ (cal/mol.K) ^c
0	70.0±0.4	-16.4±1.0	-81.2±4.5	-209.0±11.8
10	62.1±0.5	-14.3±0.7	-77.0±5.5	-202.1±10.5
20	56.2±0.6	-12.8±0.8	-76.2±4.7	-204.4±10.7
30	49.2±0.3	-11.3±1.0	-79.4±3.8	-219.4±12.3
40	41.3±0.2	-9.3±0.6	-77.9±5.3	-221.2±11.8
50 ^d	30.1±0.5	-6.1±0.5	-79.8±6.0	-237.6±11.0
100 ^e	-6.2	2.8	-78.9	-261.8
Dioxane (%)	T _m (°C) ^{b, c}	ΔG ₃₇ ⁰ (kcal/mol) ^c	ΔH ⁰ (kcal/mol) ^c	ΔS ⁰ (cal/mol.K) ^c
0	70.0±0.4	-16.4±1.0	-81.2±4.5	-209.0±11.8
10	63.0±0.6	-14.2±0.8	-74.6±3.6	-196.7±10.4
20	57.1±0.5	-13.2±0.7	-80.7±5.8	-217.8±11.6
30	53.1±0.3	-12.1±1.0	-80.2±6.2	-219.6±12.3
40	48.2±0.5	-10.7±0.6	-73.0±4.4	-200.9±10.5
50 ^f	38.3±0.2	-8.0±0.5	-74.7±4.6	-214.8±9.8
100 ^e	10.7	-1.1	-80.3	-234.8

- Thermodynamic parameters were evaluated from hyperchromicity (curve fitting) method. (Plots are in Figure 1).
- Thermal melting temperatures correspond to a DNA duplex concentration of 5.0μM in strands.
- Five independent measurements were used to calculate the standard deviation.
- Data at higher than 50% of DMF could not be obtained because of high absorption of DMF in the range of wavelength used for the experiments.
- Data obtained from manual extrapolation of the linear plots to 100% of DMF or dioxane.
- Data at higher than 50% of dioxane could not be obtained because of condensation/evaporation of dioxane at extreme temperatures.

Table S4 Comparative thermal and thermodynamic parameters^a of PNA and DNA duplexes in DMF and dioxane.

DMF (%)	T_m (°C) ^{b, c}				ΔG_{37}^0 (kcal/mol) ^c			
	PNA1·PNA2	PNA1·DNA2	PNA2·DNA1	DNA1·DNA2	PNA1·PNA2	PNA1·DNA2	PNA2·DNA1	DNA1·DNA2
0	70.2±0.3	51.3±0.4	50.8±0.2	36.3±0.5	-16.6±0.5	-10.3±1.0	-10.9±0.2	-8.2±0.7
10	68.3±0.2	47.0±0.5	46.2±0.4	29.2±0.4	-15.4±0.5	-9.5±0.7	-9.6±0.5	-6.2±1.2
20	66.2±0.2	43.1±0.3	42.1±0.3	23.7±0.5	-14.3±0.4	-9.0±0.6	-9.1±0.4	-4.9±0.8
30	64.3±0.5	40.2±0.4	39.1±0.3	18.2±0.3	-14.5±0.8	-8.3±0.6	-8.4±0.4	-3.7±0.5
40	63.4±0.3	36.2±0.5	35.0±0.5	d	-14.4±0.5	-7.7±0.8	-7.5±0.3	d
50	61.3±0.4	31.1±0.2	29.3±0.2	d	-13.6±0.7	-6.7±0.5	-6.4±0.1	d
60	60.0±0.6	f	f	f	f	f	f	f
70	56.1±0.5	f	f	f	f	f	f	f
Dioxane (%)								
0	70.2±0.3	51.3±0.4	50.8±0.2	35.8±0.5	-16.6±0.5	-10.3±1.0	-10.9±0.2	-8.2±0.7
10	69.0±0.3	48.0±0.5	e	f	-15.2±0.7	-9.8±0.8	e	f
20	68.6±0.4	45.0±0.3	e	f	-14.9±0.6	-9.2±0.9	e	f
30	68.1±0.2	41.2±0.3	e	f	-14.7±0.5	-8.6±0.7	e	f
40	67.2±0.3	39.2±0.2	e	f	-14.1±0.5	-8.1±0.6	e	f
50	66.3±0.2	34.3±0.5	e	f	-14.0±0.5	-7.5±0.8	e	f
60	65.0±0.8	f	f	f	f	f	f	f
70	61.1±0.7	f	f	f	f	f	f	f

- Thermodynamic parameters were evaluated from hyperchromicity (curve fitting) method. Plots are in Figure S4 and S5.
- Thermal melting temperatures correspond to a PNA duplex concentration of 5.0 μ M in strands.
- Five independent measurements were used to calculate the standard deviation.
- Data could not be measured because of incomplete thermal melting curves. (However, supporting data with longer DNA control DNA3·DNA4 are available. See Table S3.).
- Data were not measured because the results were obvious from the supporting data available (the other hybrid duplex).
- Data could not be measured because of poorer accuracy related to upper baseline irregularities in DMF and condensation of dioxane in the range of low temperatures required.

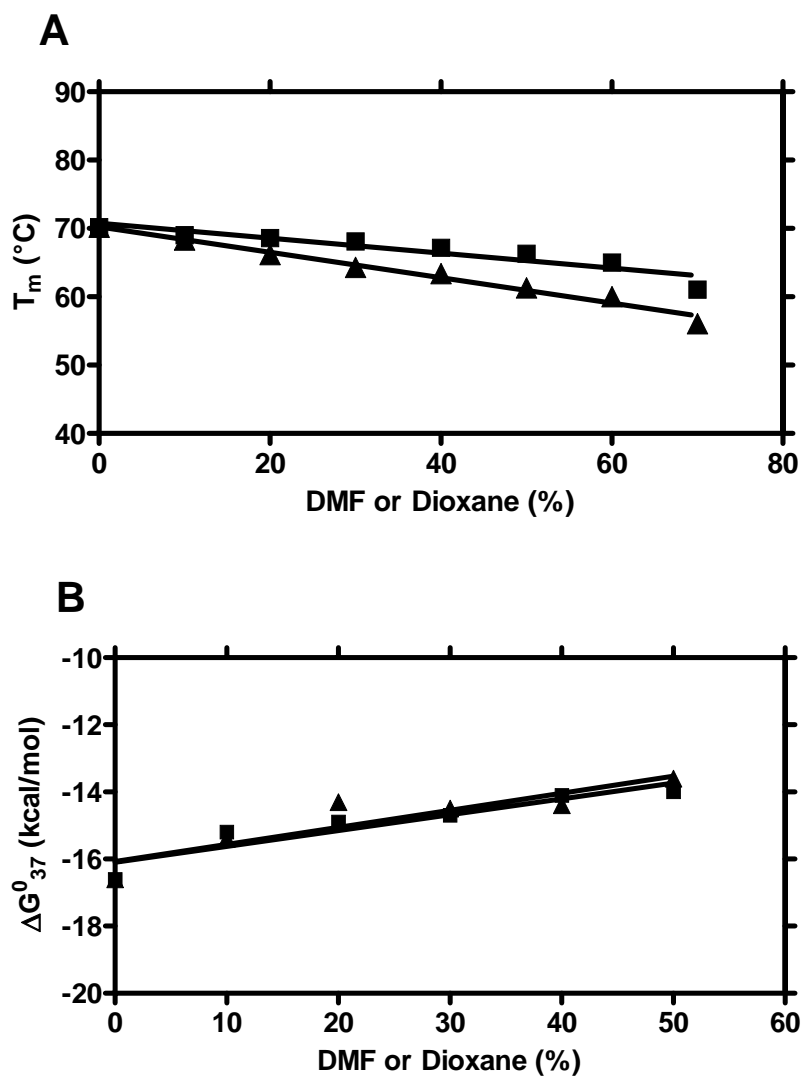


Figure S4

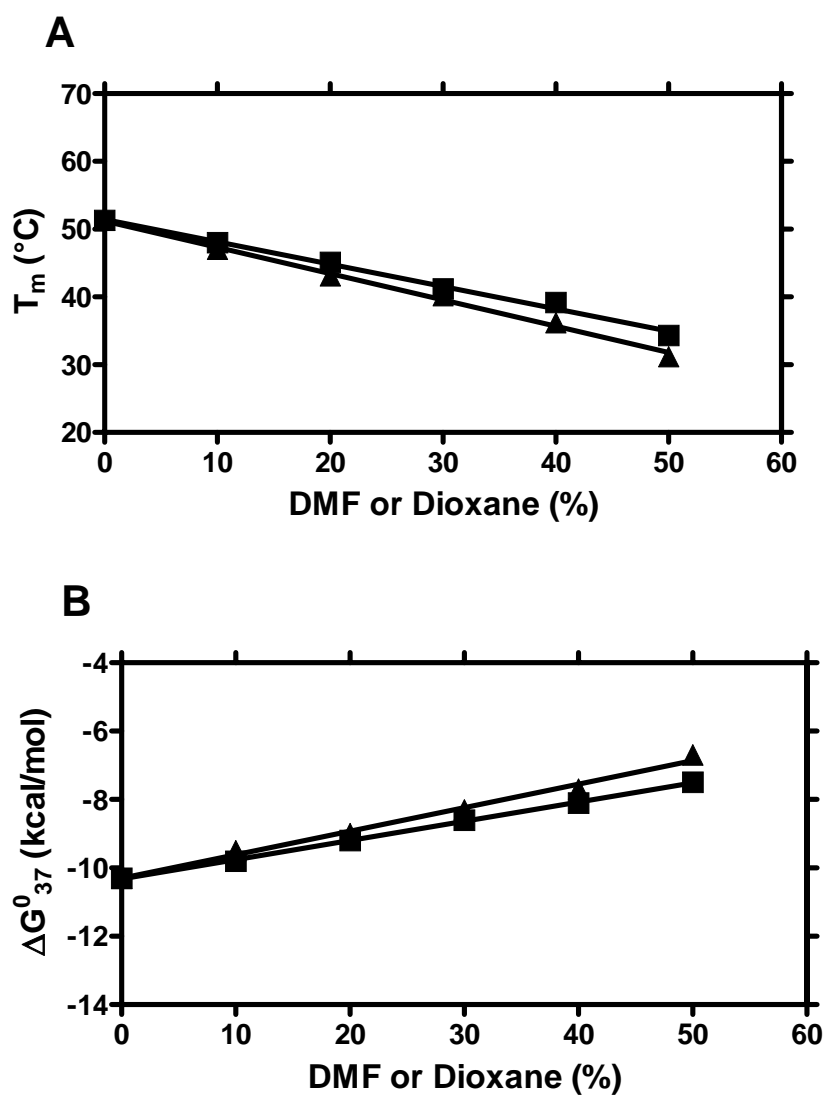


Figure S5

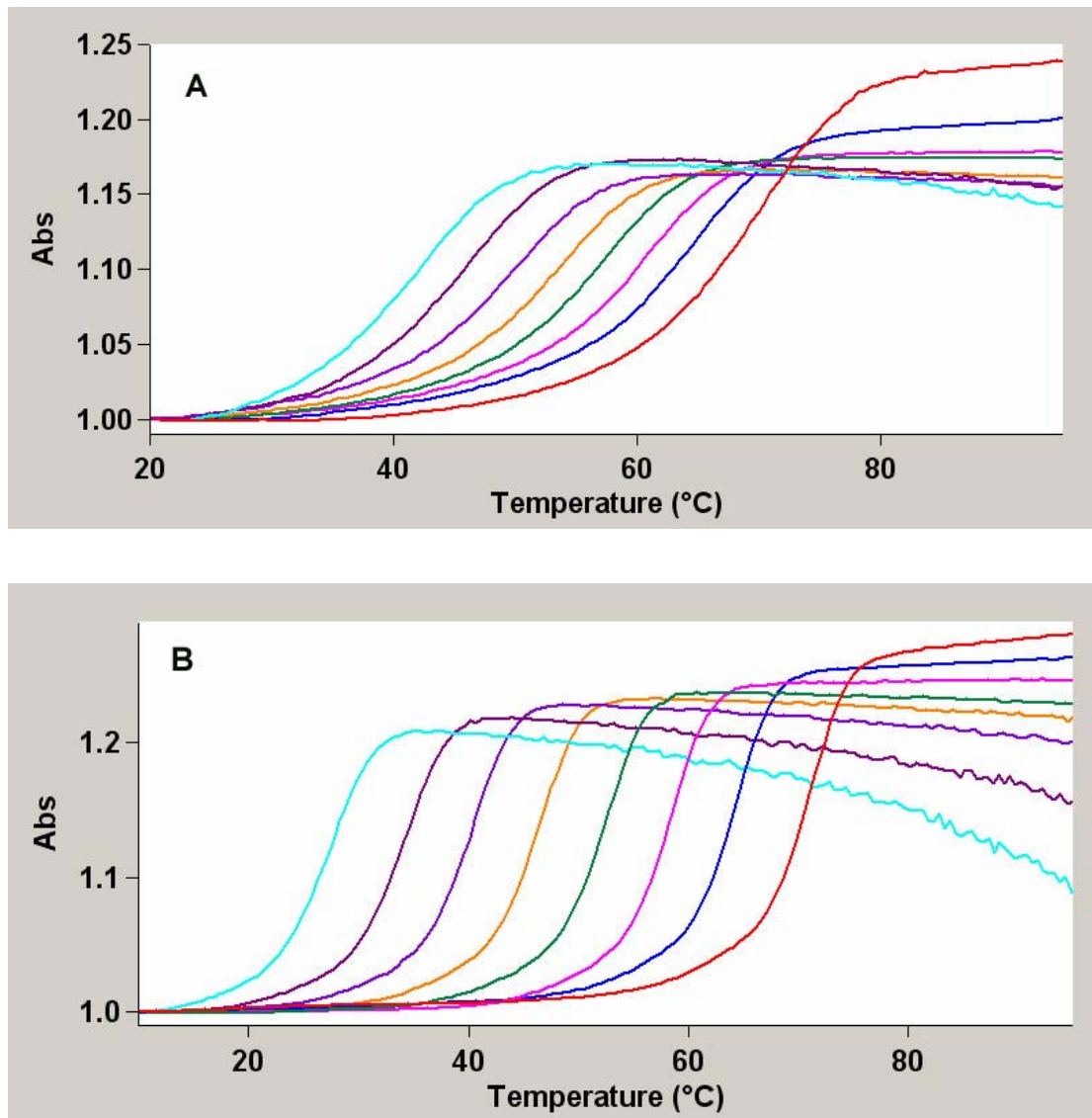


Figure S6

Table S5 Thermal and thermodynamic parameters^a of PNA and DNA duplexes in formamide.

Formamide (%)	T_m (°C) ^b		ΔG_{37}^0 (kcal/mol)		ΔH^0 (kcal/mol)		ΔS^0 (cal/mol.K)	
	PNA1·PNA2	DNA3·DNA4	PNA1·PNA2	DNA3·DNA4	PNA1·PNA2	DNA3·DNA4	PNA1·PNA2	DNA3·DNA4
0	70.0±0.08	70.0±0.4	-16.4±0.5	-16.4±1.0	-91.7±3.5	-81.2±4.5	-243.0±9.2	-209.0±11.8
10	65.1±0.04	64.1±0.7	-15.0±0.1	-14.8±0.2	-87.9±0.2	-78.6±0.3	-235.1±0.2	-206.0±1.2
20	61.1±0.03	58.2±0.5	-13.7±0.1	-13.3±0.5	-83.5±0.2	-75.4±0.6	-224.9±0.3	-200.5±3.6
30	57.2±0.03	52.3±0.5	-12.7±0.2	-11.8±0.7	-80.8±0.1	-73.1±1.3	-219.4±0.1	-197.4±4.7
40	54.0±0.05	46.0±0.6	-11.9±0.2	-10.5±0.6	-78.9±0.2	-72.5±2.0	-216.1±0.4	-200.2±2.8
50	49.1±0.06	40.1±0.8	-10.6±0.2	-8.9±0.2	-73.0±0.3	-70.8±0.4	-210.3±0.4	-199.5±2.5
60	46.1±0.05	34.2±0.7	-9.7±0.3	-7.9±0.3	-71.5±0.3	-64.4±0.7	-199.3±0.3	-182.5±6.4
70	41.2±0.04	27.3±0.6	-8.7±0.1	c	-69.2±0.2	c	-195.1±0.3	c
100 ^d	29.5	9.6	-5.4	-1.9	-58.5	-56.5	-174.5	-176.1

- Thermodynamic parameters were evaluated from hyperchromicity (curve fitting) method. (Plots are in Figures 1, S7 and S8).
- Thermal melting temperatures correspond to a PNA duplex concentration of 5.0 μ M in strands.
- Data could not be evaluated by curve fitting because of bad thermal curves and insufficient baseline.
- Data obtained from manual extrapolation of the linear graphs in Figures 1, S7 and S8.

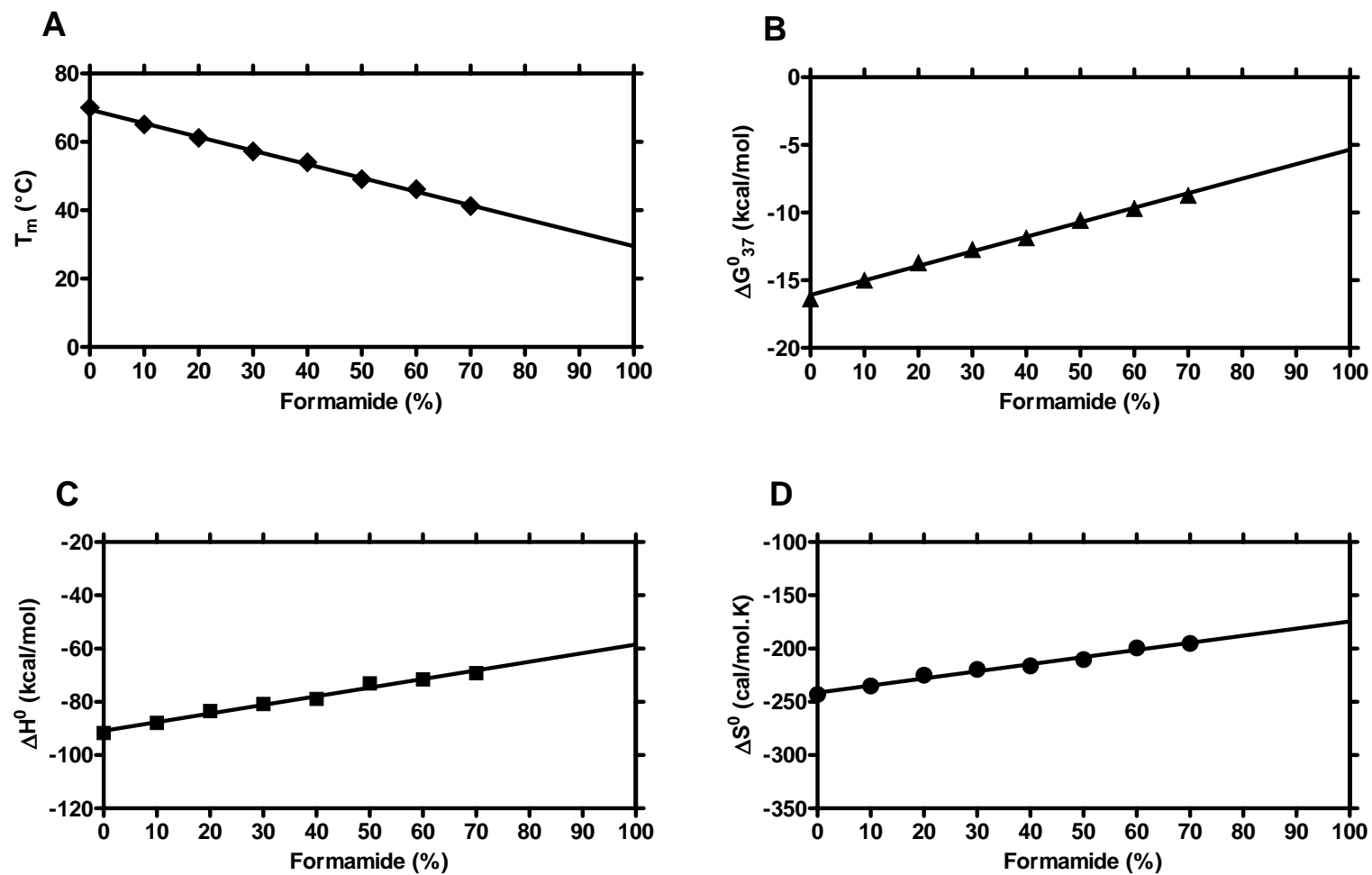


Figure S7

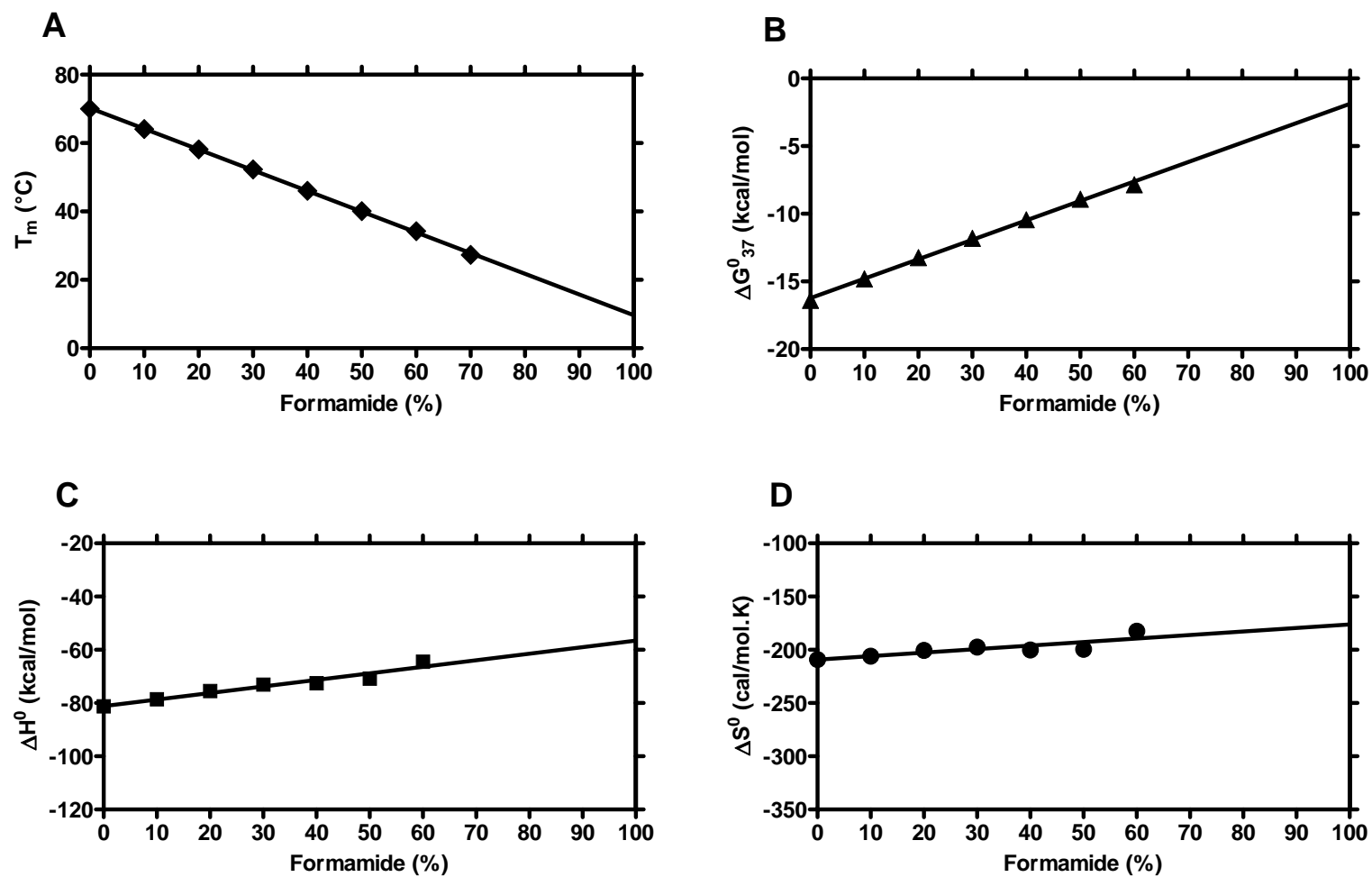


Figure S8

Table S6 Thermal and thermodynamic parameters^a of hairpin PNAs^b in DMF.

DMF (%)	T _m (°C) ^c		ΔG_{37}^0 (kcal/mol) ^c		ΔH^0 (kcal/mol) ^c		ΔS^0 (cal/mol.K) ^c	
	PNA3	PNA4	PNA3	PNA4	PNA3	PNA4	PNA3	PNA4
0	59.0±0.6	53.1±0.4	-1.6±0.5	-1.4±0.6	-29.6±5.0	-29.0±5.2	-90.2±9.6	-89.2±12.2
10	57.0±0.5	51.0±0.5	-1.9±0.7	-1.3±0.5	-32.3±5.5	-31.4±4.4	-98.2±10.7	-97.1±11.5
20	56.1±0.6	50.1±0.3	-1.9±0.7	-1.3±0.7	-34.3±6.2	-33.4±4.3	-104.4±10.2	-103.4±10.4
30	56.2±0.4	49.2±0.2	-2.0±0.8	-1.4±0.8	-36.4±4.8	-35.0±5.6	-110.7±9.3	-108.1±9.8
40	55.7±0.3	49.2±0.5	-2.2±1.0	-1.6±0.7	-40.5±4.6	-39.5±5.2	-123.4±12.0	-122.3±10.7
50	54.8±0.5	50.3±0.6	-2.3±0.5	-1.7±0.7	-43.4±5.7	-42.7±4.7	-132.6±11.6	-132.2±11.3
60	53.6±0.4	48.2±0.4	-2.2±0.5	-1.8±0.6	-45.1±5.8	-46.5±5.3	-138.0±11.8	-144.2±12.3
70 ^d	50.2±0.6 ^e	f	f	f	f	f	f	f
100 ^g	49.3	46.0	-2.7	-2.0	-55.7	-57.2	-170.6	-140.0
Slope ^g	0.09	0.06	0.01	0.01	-0.26	-0.29	-0.82	-0.90

- a. Thermodynamic parameters were evaluated from hyperchromicity (curve fitting) method. (Plots are in Figures 2A, S9A, S9B and S9C).
- b. PNA concentration was 12.0 μM in strand for PNA3 (H-AGAG-(eg1)₃-CTCT-Lys-NH₂) and 11.0 μM in strand for PNA4 (H-ACAG-(eg1)₃-CTGT-Lys-NH₂).
- c. Three independent measurements were used to calculate the standard deviation.
- d. Data could not be measured above 70% of DMF because of high absorption of DMF in the wavelength range used.
- e. Data not reliable due to bad thermal curves.
- f. Data could not be measured or evaluated due to bad thermal curves.
- g. Data were obtained from the manual extrapolations of the linear plots of Figures 2A, S9A, S9B and S9C.
- h. Data were calculated from the linear fitting of the plots of Figures 2A, S9A, S9B and S9C.

Table S7 Thermal and thermodynamic parameters^a of hairpin PNAs^b in dioxane.

Dioxane (%)	T _m (°C) ^c		ΔG ₃₇ ⁰ (kcal/mol) ^c		ΔH ⁰ (kcal/mol) ^c		ΔS ⁰ (cal/mol.K) ^c	
	PNA3	PNA4	PNA3	PNA4	PNA3	PNA4	PNA3	PNA4
0	59.0±0.5	53.0±0.4	-1.8±0.8	-1.5±0.6	-28.7±5.5	-31.7±5.2	-86.6±11.7	-97.6±11.5
10	58.0±0.4	51.0±0.5	-1.8±0.9	-1.4±0.7	-33.1±4.5	-34.5±4.6	-100.7±12.0	-106.6±10.5
20	58.1±0.6	51.2±0.3	-1.8±0.9	-1.4±0.6	-31.6±3.8	-34.6±3.7	-96.2±12.2	-106.9±12.4
30	58.1±0.3	51.1±0.4	-2.1±0.5	-1.6±0.9	-35.3±3.7	-35.6±3.9	-107.1±11.7	-109.8±10.7
40	58.2±0.4	51.2±0.6	-2.2±0.7	-1.6±0.8	-35.7±5.3	-35.2±5.4	-108.0±11.4	-108.3±10.6
50	59.3±0.3	52.3±0.5	-2.5±0.6	-1.8±0.5	-38.1±4.6	-36.5±4.5	-114.9±10.3	-111.9±11.4
60	62.1±0.2	54.1±0.4	-2.8±0.7	-2.0±0.5	-40.8±4.2	-39.3±4.8	-122.4±9.7	-120.5±10.3
70 ^{d,e}	63.2±0.4	59.1±0.3	-3.8±0.4	-2.5±0.6	-52.7±3.7	-42.5±4.4	-157.8±9.8	-129.0±9.7
100 ^f	63.8	53.4	-3.9	-2.2	-47.4	-42.2	-142.0	-129.0
Slope ^g	0.06	0.02	-0.02	-0.01	-0.18	-0.10	-0.53	-0.29

- Thermodynamic parameters were evaluated from hyperchromicity (curve fitting) method. (Plots are in Figures 2B, S9D, S9E and S9F)
- PNA concentration was 12.0 μM in strand for PNA3 (H-AGAG-(eg1)₃-CTCT-Lys-NH₂) and 11.0 μM in strand for PNA4 (H-ACAG-(eg1)₃-CTGT-Lys-NH₂).
- Three independent measurements were used to calculate the standard deviation.
- Data not reliable due to bad thermal curves.
- Data could not be measured above 70% of dioxane because of condensation/evaporation of dioxane at extreme temperatures.
- Data were obtained from the manual extrapolations of the linear plots (without taking data point for 70% dioxane into account except for T_m of PNA3) of Figures 2B, S9D, S9E and S9F.
- Data were calculated from the linear fitting of the plots (without taking the data point at 70% dioxane into account except for T_m of PNA3) of Figures 2B, S9D, S9E and S9F.

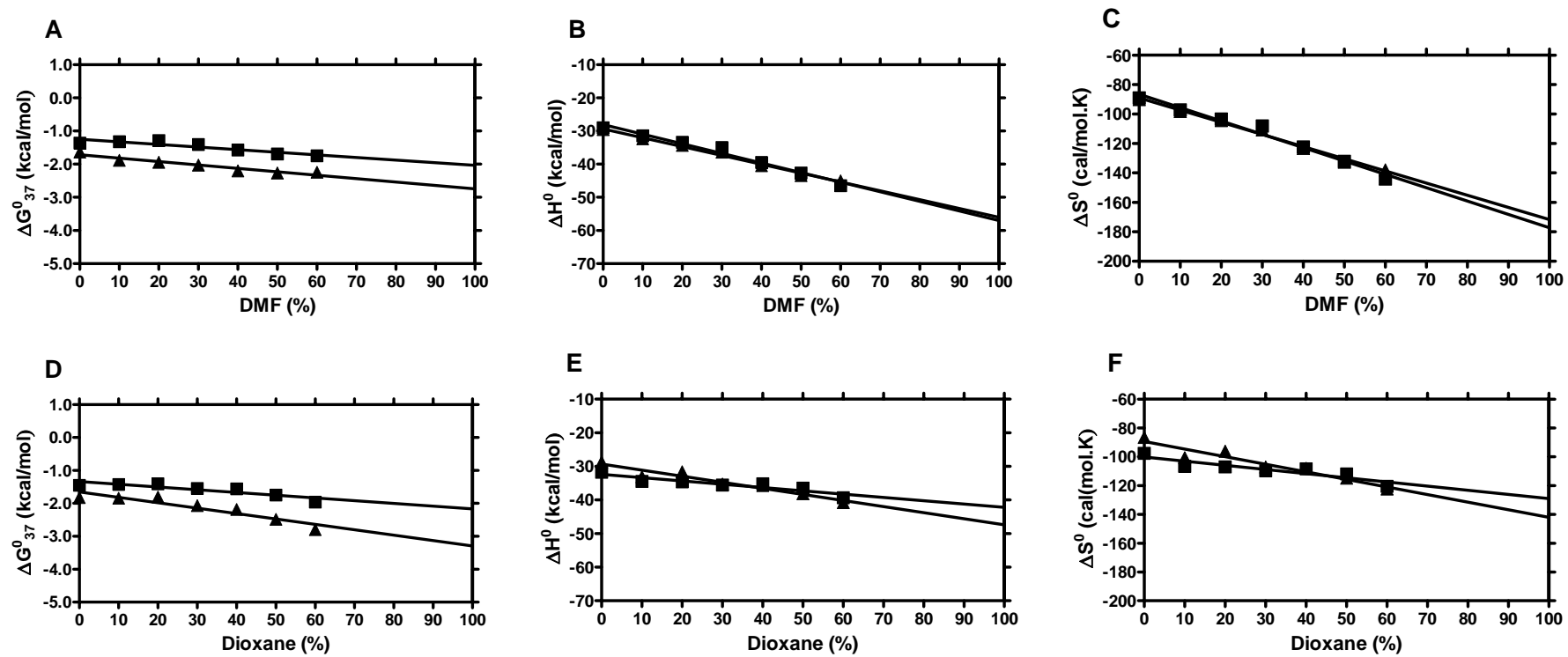


Figure S9

Table S8 Thermal and thermodynamic parameters^a of hairpin DNA control DNA5^b in DMF.

DMF (%)	T _m (°C) ^c	ΔG ₃₇ ⁰ (kcal/mol) ^c	ΔH ⁰ (kcal/mol) ^c	ΔS ⁰ (cal/mol.K) ^c
0	43.0±0.3	-0.7±0.02	-24.8±0.3	-77.7±2.5
10	34.1±0.2	-0.2±0.1	-28.2±2.0	-91.1±4.2
20	28.1±0.2	0.8±0.2 ^d	-30.5±2.2 ^d	-101.0±4.7 ^d
30	17.2±0.3	e	e	e
40 ^f	11.4±0.3	e	e	e
100 ^g	-38.7	-	-	-
Slope ^h	-0.8	-	-	-

- Thermodynamic parameters were evaluated from hyperchromicity (curve fitting) method.
- DNA concentration was 6.0 μM in strand.
- Three independent measurements were used to calculate the standard deviation.
- Data not reliable due to insufficient baseline.
- Data could not be evaluated because of incomplete thermal curves.
- Data could not be measured above 40% of DMF because of incomplete thermal curves (too low T_m).
- Data were obtained from the manual extrapolations of the linear plot of Figure S10A.
- Data were calculated from the linear fitting of the plot of Figure S10A.

Table S9 Thermal and thermodynamic parameters^a of hairpin DNA control DNA5^b in dioxane.

Dioxane (%)	T _m (°C) ^c	ΔG ₃₇ ⁰ (kcal/mol) ^c	ΔH ⁰ (kcal/mol) ^c	ΔS ⁰ (cal/mol.K) ^c
0	43.0±0.3	-0.7±0.02	-24.8±0.3	-77.7±2.5
10	38.0±0.3	-0.5±0.1	-26.8±1.5	-84.8±2.2
20	36.1±0.2	-0.1±0.1 ^d	-24.9±2.2 ^d	-80.0±3.6 ^d
30 ^d	31.2±0.4	e	e	e
40 ^f	26.3±0.4	e	e	e
100 ^g	-0.4	-	-	-
Slope ^h	3.2	-	-	-

- Thermodynamic parameters were evaluated from hyperchromicity (curve fitting) method.
- DNA concentration was 6.0 μM in strand.
- Three independent measurements were used to calculate the standard deviation.
- Data not reliable due to insufficient baseline.
- Data could not be evaluated because of incomplete thermal curves.
- Data could not be measured above 40% of dioxane because of condensation of dioxane at the range of low temperatures required.
- Data were obtained from the manual extrapolations of the linear plot of Figure S10B.
- Data were calculated from the linear fitting of the plot of Figure S10B.

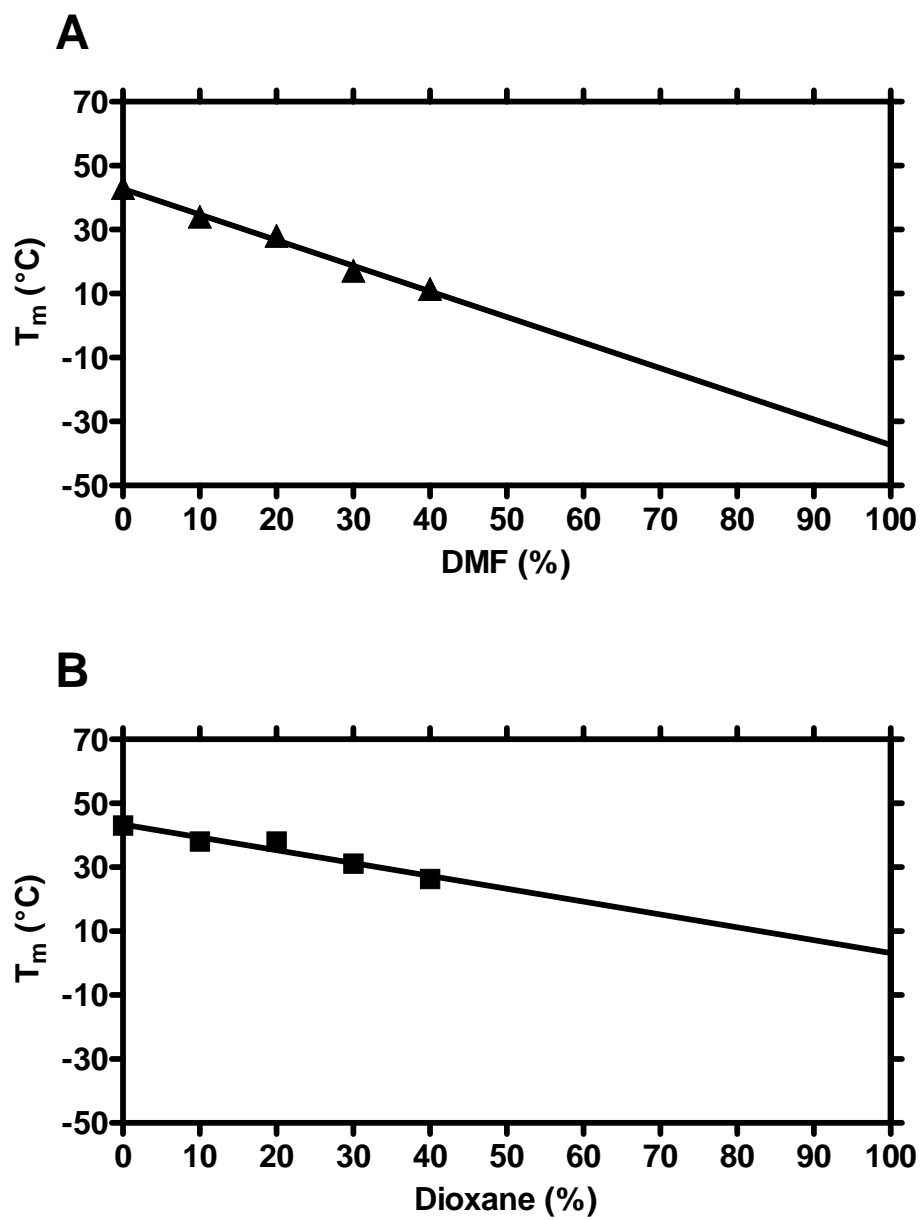


Figure S10

Table S10 Thermal and thermodynamic parameters^a of PNA duplexes containing tricyclic thymine (tT) and its control duplex in DMF.

PNA duplex	DMF (%)	T _m (°C) ^{b, c}	ΔG ₃₇ ⁰ (kcal/mol) ^c
PNA5/PNA6 ^d	0	75.0±0.57	-15.2±0.3
	10	72.1±0.50	-14.8±0.1
	20	70.1±0.50	-16.1±0.2
	30	67.2±0.56	-15.6±0.2
	40	66.0±0.01	-15.6±0.5
	50	63.1±0.01	-14.7±0.5
	60	61.2±0.01	-13.7±0.8
	70	57.2±0.6	e
	100 ^f	50.9	-13.8
PNA6/PNA7 ^d	0	69.0±0.01	-14.2±0.3
	10	67.1±0.57	-14.3±0.2
	20	66.2±0.01	-15.2±0.3
	30	64.2±0.56	-15.4±0.9
	40	64.0±0.60	-15.5±1.0
	50	62.1±0.01	-14.5±0.6
	60	60.2±0.01	-14.0±0.6
	70	58.3±0.57	e
	100 ^f	54.4	-14.6

- Thermodynamic parameters were evaluated from hyperchromicity (curve fitting) method.
- Thermal melting temperatures correspond to a PNA duplex concentration of 5.0 μM in strands.
- Three independent measurements were used to calculate the standard deviation.
- PNA5 is H-tT-GTA GAT CAC T-NH₂, PNA6 is H-AGT GAT CTA C-NH₂ and PNA7 is H-GTA GAT CAC T-NH₂.
- Data could not be evaluated by curve fitting because of bad thermal curves.
- Data obtained from manual extrapolation of the linear graphs in Figure S11.

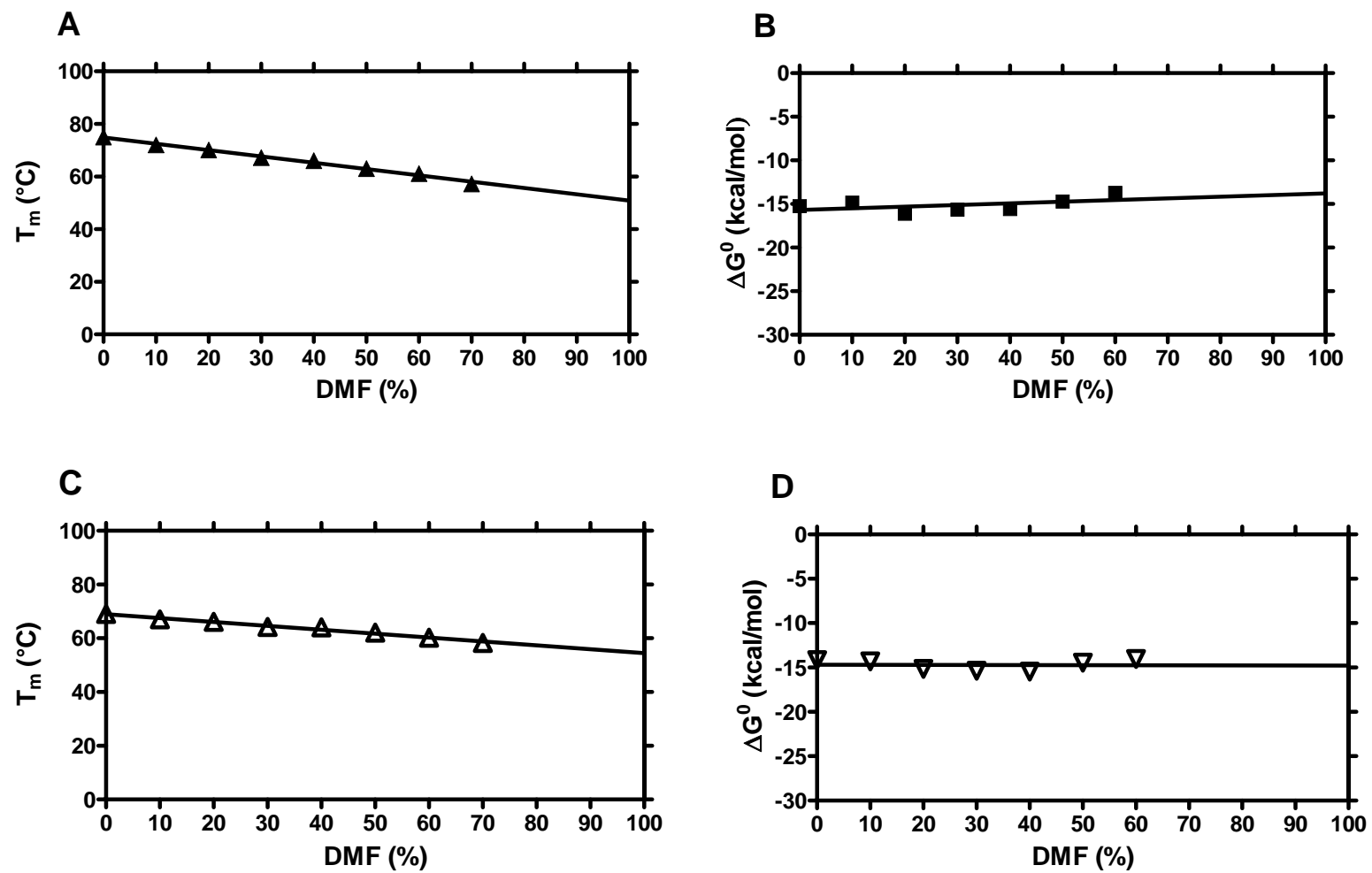


Figure S11

Table S11 Thermal and thermodynamic parameters^a of single base mismatched PNA duplexes in DMF.

PNA duplex	DMF (%)	T _m (°C) ^{b, c}	ΔG ₃₇ ⁰ (kcal/mol) ^c
PNA1/PNA8 ^d (T·T mismatch)	0	53.0±0.03	-10.0±0.04
	10	51.0±0.02	-10.2±0.04
	20	49.1±0.02	-10.1±0.03
	30	48.2±0.03	-9.9±0.01
	40	47.0±0.01	-9.7±0.02
	50	46.1±0.05	-9.5±0.05
	60	45.2±0.06	-9.3±0.02
	70 ^e	41.3	-8.5
	100 ^f	39.7	-8.9
PNA2/PNA9 ^d (A·A mismatch)	0	54.0±0.01	-11.0±0.05
	10	52.1±0.02	-10.8±0.06
	20	52.1±0.01	-10.7±0.04
	30	52.2±0.03	-10.3±0.05
	40	51.0±0.02	-10.6±0.05
	50	50.1±0.01	-10.9±0.02
	60	49.2±0.01	-10.3±0.03
	70 ^e	45.3	-9.6
	100 ^f	46.7	-10.2
PNA2/PNA10 ^d (C·T mismatch)	0	52.0±0.01	-10.3±0.06
	10	51.0±0.05	-10.5±0.05
	20	50.1±0.05	-10.5±0.01
	30	49.2±0.06	-10.5±0.02
	40	48.0±0.01	-10.5±0.02
	50	47.1±0.01	-10.6±0.05
	60	45.1±0.02	-10.0±0.01
	70 ^e	41.2	-8.8
	100 ^f	41.3	-10.2

- Thermodynamic parameters were evaluated from hyperchromicity (curve fitting) method.
- Thermal melting temperatures correspond to a PNA duplex concentration of 5.0μM in strands.
- Three independent measurements were used to calculate the standard deviation.
- PNA8 is H-AGT GTT CTA C-Lys-NH₂, PNA9 is H-GTA GAA CAC T-Lys-NH₂ and PNA10 is H-GTA GCT CAC T-Lys-NH₂.
- Data not reliable because of bad thermal curves.
- Data obtained from manual extrapolation of the linear graphs in Figures S12 and S13 (without taking the data point at 70%DMF into account).

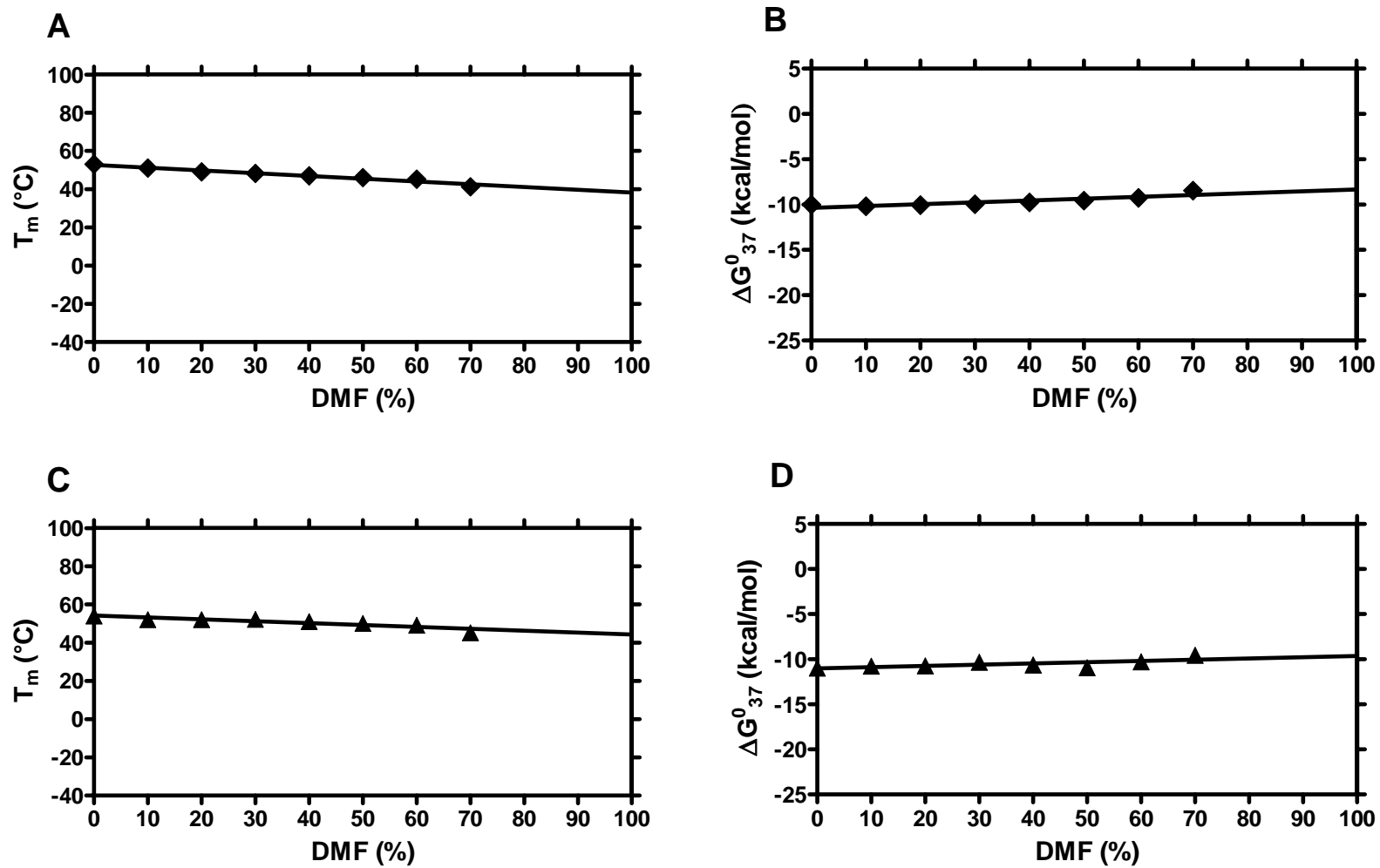


Figure S12

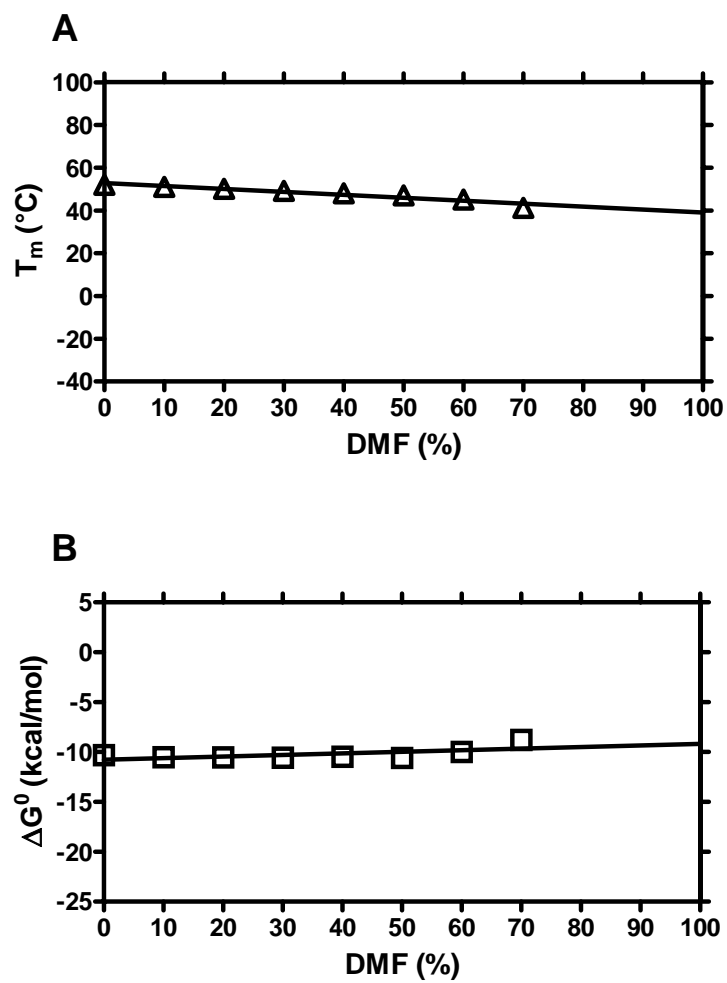


Figure S13

Figure legends

Figure S1 Representative thermal melting curves of PNA1·PNA2 (red), PNA1·DNA2 (blue), PNA2·DNA1 (green), DNA1·DNA2 (violet) and DNA3·DNA4 (orange) in pure aqueous buffer (10 mM phosphate buffer containing 100 mM NaCl and 0.1 mM EDTA, pH 7.2±0.01).

Figure S2 (A) Representative thermal melting curves of PNA1·PNA2 in 10% DMF (red), 20% DMF (blue), 30% DMF (pink), 40% DMF (green) and 50% DMF (orange). (B) Representative thermal melting curves of PNA1·PNA2 in 10% dioxane (red), 20% dioxane (blue), 30% dioxane (pink), 40% dioxane (green) and 50% dioxane (orange).

Figure S3 (A) Representative thermal melting curves of DNA3·DNA4 in 0% DMF (red), 10% DMF (blue), 20% DMF (pink), 30% DMF (green), 40% DMF (orange) and 50% DMF (violet). (B) Representative thermal melting curves of DNA3·DNA4 in 0% dioxane (red), 10% DMF (blue), 20% dioxane (pink), 30% dioxane (green), 40% dioxane (orange) and 50% dioxane (violet).

Figure S4 Comparison of thermal stabilities of PNA1·PNA2 in DMF and dioxane. Plots of (A) thermal melting temperature (T_m) and (B) Gibbs' free energy change (ΔG_{37}^0) of PNA1·PNA2 as a function of the amount of DMF (—▲—) and dioxane (—■—) in the medium. The aqueous buffer was 10 mM phosphate buffer containing 100 mM NaCl and 0.1 mM EDTA, pH 7.2±0.01.

Figure S5 Comparison of thermal stabilities of PNA1·DNA2 in DMF and dioxane. Plots of (A) thermal melting temperature (T_m) and (B) Gibbs' free energy change (ΔG_{37}^0) of PNA1·DNA2 as a function of the amount of DMF (—▲—) and dioxane (—■—) in the medium. The aqueous buffer was 10 mM phosphate buffer containing 100 mM NaCl and 0.1 mM EDTA, pH 7.2±0.01.

Figure S6 (A) Representative thermal melting curves of PNA1·PNA2 in pure aqueous buffer (red), 10% formamide (blue), 20% formamide (pink), 30% formamide

(green), 40% formamide (orange), 50% formamide (violet), 60% formamide (magenta) and 70% formamide (teal). (B) Thermal melting curves of DNA3·DNA4 in pure aqueous buffer (red), 10% formamide (blue), 20% formamide (pink), 30% formamide (green), 40% formamide (orange), 50% formamide (violet), 60% formamide (magenta) and 70% formamide (teal).

Figure S7 Thermal and thermodynamic data of PNA duplexes in formamide. Plots of (A) thermal melting temperature (T_m) (—◆—), (B) Gibbs' free energy change (ΔG_{37}^0) (—▲—), (C) enthalpy change (ΔH^0) (—■—) and (D) entropy change (ΔS^0) (—●—) of PNA1·PNA2 as a function of the amount of formamide in the medium. The aqueous buffer was 10 mM phosphate buffer containing 100 mM NaCl and 0.1 mM EDTA, pH 7.2 ± 0.01 .

Figure S8 Thermal and thermodynamic data of DNA duplexes in formamide. Plots of (A) thermal melting temperature (T_m) (—◆—), (B) Gibbs' free energy change (ΔG_{37}^0) (—▲—), (C) enthalpy change (ΔH^0) (—■—) and (D) entropy change (ΔS^0) (—●—) of DNA3·DNA4 as a function of the amount of formamide in the medium. The aqueous buffer was 10 mM phosphate buffer containing 100 mM NaCl and 0.1 mM EDTA, pH 7.2 ± 0.01 .

Figure S9 Plots of thermodynamic data of hairpin PNAs in DMF and dioxane. Plots of (A) Gibbs' free energy change (ΔG_{37}^0), (B) enthalpy change (ΔH^0) and (C) entropy change (ΔS^0) of PNA3 (—◆—) and PNA4 (—■—) as a function of the amount of DMF in the medium. Plots of (D) Gibbs' free energy change (ΔG_{37}^0), (E) enthalpy change (ΔH^0) and (F) entropy change (ΔS^0) of PNA3 (—◆—) and PNA4 (—■—) as a function of the amount of dioxane in the medium. The aqueous buffer was 10 mM phosphate buffer containing 100 mM NaCl and 0.1 mM EDTA, pH 7.2 ± 0.01 .

Figure S10 Thermal stabilities of hairpin DNA control DNA5 in DMF and dioxane. Plots of T_m values of DNA5 as a function of the amount of (A) DMF

(—▲—) and (B) dioxane (—■—) in the medium. The aqueous buffer was 10 mM phosphate buffer containing 100 mM NaCl and 0.1 mM EDTA, pH 7.2±0.01.

Figure S11 Thermal stabilities of tT-PNA duplex in DMF compared to its unmodified control. Plots of (A) thermal melting temperature (T_m) (—▲—) and (B) Gibbs' free energy change (ΔG_{37}^0) (—■—) of PNA5·PNA6 as a function of the amount of DMF in the medium. Plots of (C) thermal melting temperature (T_m) (—△—) and (D) Gibbs' free energy change (ΔG_{37}^0) (—▽—) of PNA6·PNA7 as a function of the amount of DMF in the medium. The aqueous buffer was 10 mM phosphate buffer containing 100 mM NaCl and 0.1 mM EDTA, pH 7.2±0.01.

Figure S12 Thermal stabilities of T·T and A·A mismatched PNA duplexes in DMF. Plots of (A) thermal melting temperature (T_m) and (B) Gibbs' free energy change (ΔG_{37}^0) of PNA1·PNA8 (—◆—) as a function of the amount of DMF in the medium. Plots of (C) thermal melting temperature (T_m) and (D) Gibbs' free energy change (ΔG_{37}^0) of PNA2·PNA9 (—▲—) as a function of the amount of DMF in the medium. The aqueous buffer was 10 mM phosphate buffer containing 100 mM NaCl and 0.1 mM EDTA, pH 7.2±0.01.

Figure S13 Thermal stabilities of C·T mismatched PNA duplexes in DMF. Plots of (A) thermal melting temperature (T_m) (—△—) and (B) Gibbs' free energy change (ΔG_{37}^0) (—□—) of PNA2·PNA10 as a function of the amount of DMF in the medium. The aqueous buffer was 10 mM phosphate buffer containing 100 mM NaCl and 0.1 mM EDTA, pH 7.2±0.01.